International Journal of Applied Science and Engineering
2009. 7, 2: 133-142

Electrical Energy Generated by a Photovoltaic Module Installed on East-West Tracked Panel

Tian Pau Chang*

Department of Computer Science and Information Engineering, Nankai University of Technology, Nantou 542, Taiwan

Abstract: The research concerning a tracked panel oriented in the east-west (EW) direction has seldom been found in literature. This paper simulates the electrical energy output from a photovoltaic (PV) module mounted on the EW-tracked panel in Taipei according to both the solar radiation observed and the radiation under clear sky condition predicted by an empirical model; subsequently the gain of the tracked panel relative to a fixed horizon panel can be analyzed. The results show that the tracked panel captures more radiation near solar noon, irrespective of date, for the smallest incident angle of sunlight at noon, which is helpful to a design focusing power supply on the noon particularly. As compared to a fixed horizon panel the tracked panel makes a greater gain in winter but worse in summer. The annual output energy from the tracked panel is 228.2 and 82.1 kWh/m^2, for the clear sky and observed radiation, respectively, having the conversion efficiency of 9.1% and 8.2% respectively. The output energy increases with the maximum rotation angle of tracked panel, but the benefit of applying a tracking system in real environment as in Taipei is not as good as in clear sky condition. With the maximum rotation angle of 45^o, the yearly gains of output energy obtained by the tracked panel are 14.1% and 5.5% for the clear sky and observed radiation, respectively.

Keywords: Solar radiation; EW-tracked panel; Photovoltaic module; Gain.

1. Introduction

Solar energy is currently the most important renewable energy source because of its abundance and accessibility. It can be converted into electric power through solar cell with photovoltaic (PV) effect. PV module is composed of several solar cells. The output power of a PV module depends mainly on two factors, i.e. cell temperature and solar radiation incident on it. When the cell temperature increases, the open circuit voltage of solar cell will decrease that leads to the reduction of maximum power. While the solar radiation increases, the short circuit current, maximum power and conversion efficiency will increase [1]. Figure 1 shows the equivalent circuit of a solar cell consisting of a current generator in parallel with a resistor-diode network [2]. The photo-induced current I_{ph} is proportional to the intensity of solar radiation S (in kW/m^2) expressed as [3]:

$$I_{ph} = [I_{scr} + C_i \frac{T - T_r}{1000}]\, S \tag{1}$$

* Corresponding author; e-mail: t118@nkut.edu.tw
Accepted for Publication: March 11, 2010,

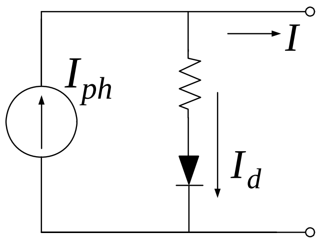

Figure 1. Equivalent circuit of a solar cell

Where T is the cell temperature, T_r is reference temperature, I_{scr} is short circuit current under the reference operating conditions (i.e. 1 kW/m^2, AM 1.5, 25^{o}C). C_i is the temperature coefficient of short circuit current. To estimate the cell temperature from ambient temperature T_a, the empirical correlation presented in Markvart [4] is adopted:

$$T = T_a + \frac{NOCT - 20}{0.8} S \qquad (2)$$

Where NOCT is the normal operating cell temperature. Assuming that the shunt resistance of a solar cell is infinite, so the current in the shunt resistance can be neglected, the current through the bypass diode I_d and the reverse saturation current I_{sat} can be calculated as:

$$I_d = I_{sat}[\exp(\frac{qV}{KAT}) - 1] \qquad (3)$$

$$I_{sat} = I_{rr}(\frac{T}{T_r})^3 \exp[\frac{qE_g}{KA}(\frac{1}{\mathrm{T_r}} - \frac{1}{\mathrm{T}})] \qquad (4)$$

Where, q is the magnitude of electron charge, V is output voltage, K is the Boltzmann constant, A is ideality factor, I_{rr} is diode reverse saturation current at reference temperature, E_g is semiconductor gap energy. The output current I can be calculated by:

$$I = I_{ph} - I_d \qquad (5)$$

Figure 2 demonstrates the characteristic curves (*I*-*V* and *P*-*V*) of mono-crystalline silicon solar cell at the reference operating conditions. The electrical specifications used in the simulation of the present study are referred from SIEMENS-SP75, which is a popular device in solar market [5], with the maximum power 75W at the point of 17V, 4.4A as given in Table 1. Subsequently the accumulated output energy at the maximum power point over a given period of time can be determined.

Table 1. Electrical specifications (1 kW/m^2, AM 1.5, 25^{o}C)

Number of cells in series	36
Nominal maximum power (W)	75
Maximum power current (A)	4.4
Maximum power voltage (V)	17
Short circuit current (A)	4.75
Open circuit voltage (V)	21.7
Temperature coefficient (mA/ ^{o}K)	1.7
Reverse saturation current (A)	10^{-9}
Ideality factor	1.03
Gap energy (eV)	1.1

The best way to collect more solar radiation is to use a tracking system because it is aimed at the Sun with a smaller incident angle of sunlight [6-7]. The amount of extra energy collected by a tracked panel depends on the specific application and local weather conditions. Generally speaking, the benefits are about 20%~40% higher than for a traditional fixed panel. Huang and Sun [8] designed a single-axis three-position tracking system, adjusting PV's position only at three fixed angles, i.e. during the morning, noon and afternoon.

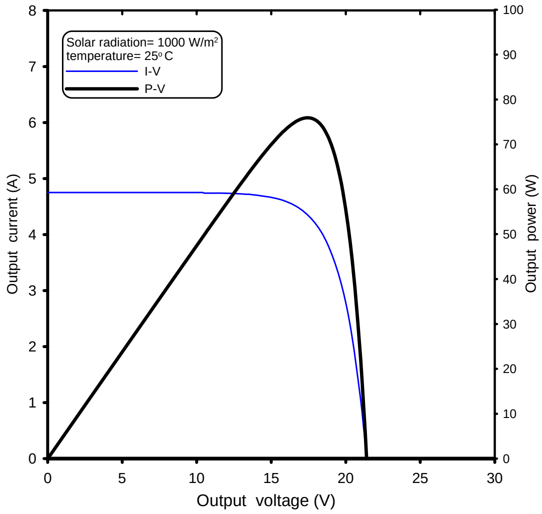

Figure 2. Characteristic curves of solar cell at reference condition

They concluded that the best stopping angle during the morning or afternoon was about 50^o from the solar noon position, irrespective of latitude, and there was 24.5% more power generation than a fixed PV module. Abdallah [9] performed an experimental study to investigate the effect of using different types of Sun tracking systems on the electrical power generation, and found there were gains of electrical power up to 43.87%, 37.53%, 34.43% and 15.69% for the two axes, east–west, vertical and north–south tracking, respectively, as compared with the fixed surface inclined 32° to the south in Jordan. The gain of a tracked-panel is defined as the enhancement of energy obtained using the tracked-panel for a given time period divided by the energy obtained using a fixed-panel for the same time period. Al-Mohamad [10] designed a Sun tracking system using a programmable logic-controller unit to control and monitor the mechanical movement of PV module. It is found that the daily output power of the PV was increased by more than 20% in comparison with that of a fixed module. Sungur [11] proposed a similar result with that of Abdallah [9] that there is 42.6% energy gain obtained by a two-axes Sun tracking system in Turkey.

Taiwan is situated between the world's largest continent (Asia) and the largest ocean (Pacific). The Tropic of Cancer (23.5° N) divides roughly the island into two climates: the tropical monsoon climate in the south and the subtropical monsoon climate in the north. The latitude and topography, ocean currents and monsoons are the main contributing factors [12]. In summer, high temperature and humidity, massive rainfall and tropical cyclones characterize the climate of Taiwan. In winter, when the northeastern monsoon system is active, the north is constantly visited by drizzle while the south remains dry. In spring, the weather in the north is rainy, leading to weaker solar radiation, e.g. in Taipei.

The research concerning Taiwan is few in literature additionally the performance analysis relevant to an east-west oriented single axis tracked panel (namely EW-tracked panel hereafter), on the basis of PV's output energy, has never been found so far. In the present study, the mathematic expressions applicable to calculate the solar radiation upon the EW-tracked panel are addressed. To simulate various operation conditions to a solar device, both the radiation observed in Taipei ($\phi=25^oN$) and the radiation predicted by an empirical model that may be considered as worldwide average in clear sky condition will be taken into account. As stated in previous studies, the discrepancy between clear sky radiation and observed one could be attributed to the attenuation of local clouds or aerosols [13-15]. The meteorological data used is averaged from 1990 to 1999 recorded by the Central Weather Bureau Taiwan. Where, the pyranometer is made by Eppley Laboratory that measures the total band of shortwave radiations (wavelength of 280-2800 nm). Finally the electrical energy output from PV module mounted on EW-tracked panel and the relevant gains of the panel will be investigated.

2. Motion of EW-tracked panel

In spherical coordinate system the Sun's position can be indicated by unit vector $\vec{P}$ [16]:

$$\vec{P} = \sin\theta_z \cos\psi\ \vec{i} + \sin\theta_z \sin\psi\ \vec{j} + \cos\theta_z\ \vec{k} \qquad (6)$$

Where θ_z is the zenith angle, ψ is the azimuth of the Sun measured from due south positive in the morning and negative in the afternoon [4]

$$\cos\theta_z = \sin\delta \sin\phi + \cos\delta \cos\phi \cos\omega \qquad (7)$$

$$\cos\psi = (\cos\theta_z \sin\phi - \sin\delta)\ /\sin\theta_z \cos\phi \qquad (8)$$

Where ϕ is the geographic latitude, ω is the solar hour angle which changes by 15 degrees per hour, and is zero at solar noon, negative in the morning and positive in the afternoon (e.g. –45^o for 9AM and +30^o for 2PM). The solar declination, δ, is the angle between the line joining the centers of the Earth, Sun and the equatorial plane, and can be given by:

$$\delta = 23.45 \sin(2\pi(284 + dn)/365.25) \qquad (9)$$

Where dn is the day number counted from January 1st throughout the year (1-365).

As shown in Fig. 3, a PV module or solar collector is installed on EW-tracked panel that may rotate only southward (or northward) about its axis through an angle γ from the horizon, the unit normal vector of the collector panel is expressed as:

$$\vec{M} = \sin\gamma\ \vec{i} + 0\ \vec{j} + \cos\gamma\ \vec{k} \qquad (10)$$

γ is positive when rotating southward, negative northward, and 0^o while the panel is in horizon.

Meanwhile, another unit vector, $\vec{M}'$, which is parallel to the panel and perpendicular to the normal vector, lagged behind the normal vector by 90^o when rotating, can be expressed as:

$$\vec{M}' = \sin(\gamma - 90)\ \vec{i} - 0\ \vec{j} + \cos(\gamma - 90)\ \vec{k} \qquad (11)$$

As the Sun moves through the sky, the solar device will collect the most energy when the vector $\vec{M}'$ is perpendicular to $\vec{P}$. Thus, the angle γ that the tracking system has to rotate to face the Sun can be determined from the fact that the scalar product $\vec{P} \cdot \vec{M}' = 0$, then:

$$\gamma = \tan^{-1}(\tan\theta_z \cos\psi) \qquad (12)$$

From this, the instantaneous incident angle of sunlight upon the track panel, θ_{ew}, can be calculated using the scalar product between $\vec{P}$ and $\vec{M}$:

$$\theta_{ew} = \cos^{-1}(\sin\theta_z \cos\psi \sin\gamma + \cos\theta_z \cos\gamma) \qquad (13)$$

The rotation angle of a sun-tracking system must be limited to avoid damage from high winds in practical design. During the simulation of the present study, the maximal rotation angle was set to be 45^o in both the southward and northward directions.

3. Solar radiation upon a tracked panel

For a particular area, solar radiation incident to the ground surface under clear sky condition can be predicted through empirical equations [6, 8]. As shown in Figure. 3, both the slope of the panel and the incident angle of sunlight change with time, the global radiation (I_t) incident on a tilted panel is composed of the direct beam, diffuse and reflection from the ground surface and can be expressed as:

$$I_t = I_{cb} R_b + I_{cd} (1+\cos\gamma)/2 + I_c\,\rho\,(1-\cos\gamma)/2 \qquad (14)$$

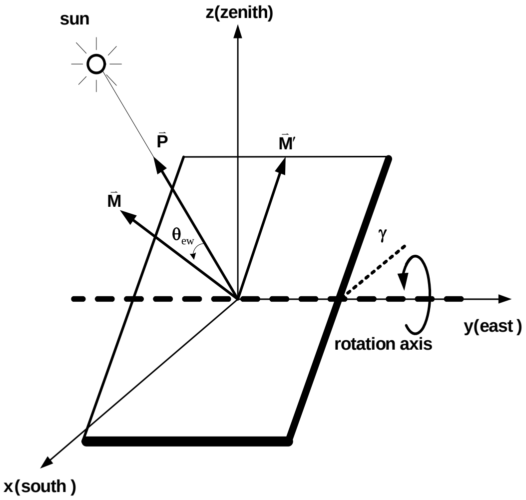

Figure 3. Geometry of East-West oriented single axis tracked panel

Where I_{cb} and I_{cd} are the beam and diffuse radiation, respectively, on a horizontal surface under clear sky. I_c is the sum of I_{cb} and I_{cd}:

$$I_c = I_{cb} + I_{cd} \qquad (15)$$

ρ is the ground reflection coefficient. R_b is the ratio of beam radiation on the tilted panel to that on a horizontal surface given as:

$$R_b = \cos\theta_{ew} / \cos\theta_z \qquad (16)$$

The observation data available in this paper is given in the form of daily global irradiance on the horizontal ground surface, i.e. the accumulated global radiation during the day. Corresponding expressions could be used to estimate the instantaneous radiation from the accumulated data [17], their appropriateness has already been analyzed in [18]; the instantaneous solar radiation on the tracked panel can be thus determined.

4. Results and discussion

Figure 4 and 5 show the EW-tracked panel's performance during the autumnal equinox and winter solstice day, respectively, according to the predicted radiation under clear sky condition. As compared to a fixed horizon panel, the EW-tracked panel receives more radiation especially near solar noon because the incident angle of sunlight upon the panel is always 0^o at noon.

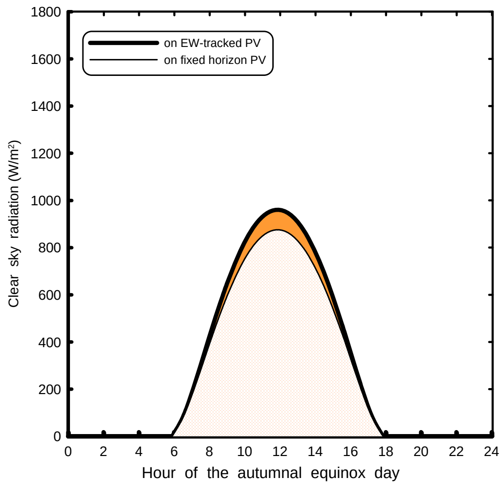

Figure 4. Clear sky radiation on EW-tracked panel during the autumnal equinox

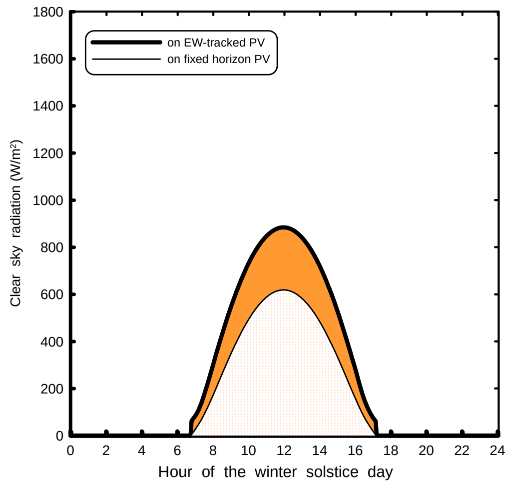

Figure 5. Clear sky radiation on EW-tracked panel during the winter solstice

This characteristic differs from that of north–south tracked panel as in Chang [18], and is useful in practical designs focusing particularly on the power supply near noon. Similar trends are also found in the case of observation data, i.e. in Figure. 6 and 7, but with a lower gain for the tracked panel due to the weaker radiation intensity actually observed; the radiation upon EW-tracked panel reveals only a little higher than that upon fixed horizon panel during the day. As a result, the curve of the tracked panel almost superimposed that of the fixed panel. Note that the EW-tracked panel achieves a better performance on the winter solstice day than on any other days due to the lowest Sun's elevation. Annual gains achieved by the tracked panel for different radiation sources are listed in Table 2.

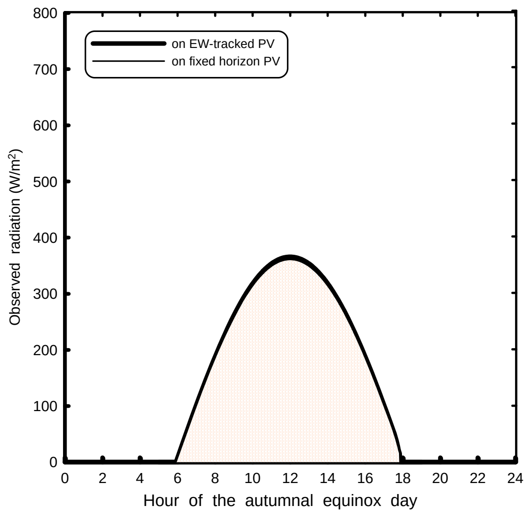

Figure 6. Observed radiation on EW-tracked panel during the autumnal equinox

Figure 8 and 9 illustrate the daily output energy of PV mounted on EW-tracked panel throughout the year calculated from clear sky and observed radiations, respectively. The irradiance incident upon a fixed horizontal PV is plotted too.

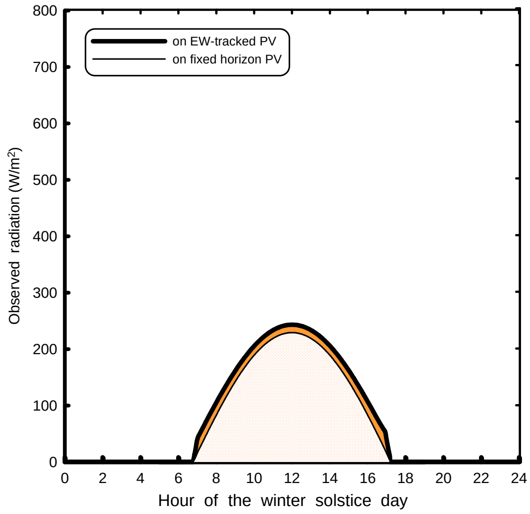

Figure 7. Observed radiation on EW-tracked panel during the winter solstice

Solar cell temperature is estimated using the environment temperature reported by the Central Weather Bureau; its monthly average is shown in Figure 10. As seen the observed irradiance is far less than the clear sky one resulting from local climatic factors, additionally the electrical energy generated by tracked PV is just a little greater than that by fixed PV and so it is hard to distinguish each other (in Figure 9). It is also found that, relative to a fixed horizon PV, the output energy from tracked PV reveals a greater value in winter months accompanied with a higher gain, independent of radiation sources. The gain is worse in summer due to the higher elevation of the Sun in this season, which is advantageous to energy collection of a horizontal panel. On the other hand, as concluded by Chang [18], the annual gains of a north–south tracked-panel reach as high as 36.0% and 15.4% for clear sky and observed radiations, respectively, due to its different movement mechanism. However the EW-tracked panel proposed still has its superiorities in specific application situation.

Table 2. Annual solar irradiance and electrical energy (kWh/m2) for different panels

	Radiation	Fixed horizon panel	EW-tracked panel	Gain (%)
Solar irradiance	Clear sky	2189.6	2496.0	**14.0**
	Observed	952.1	1002.5	**5.3**
Electrical energy	Clear sky	200.0	228.2	**14.1**
	Observed	77.8	82.1	**5.5**

As summarized in Table 2, the annual electrical energy obtained by the EW-tracked PV is 228.2 and 82.1 kWh/m^2, for the clear sky and observed radiation, respectively. The yearly conversion efficiency of PV is 9.1% and 8.2% for clear sky and observed radiation, respectively. Overall the simulation results of the present work are consistent with the experimental results of Hussein et al. [19] by using the same type of solar cell.

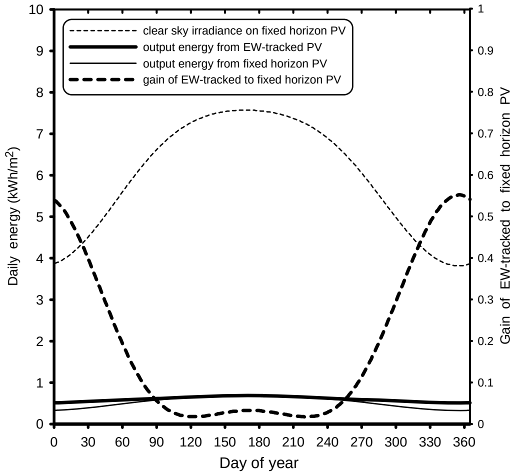

Figure 8. EW-tracked PV's daily performance according to clear sky radiation

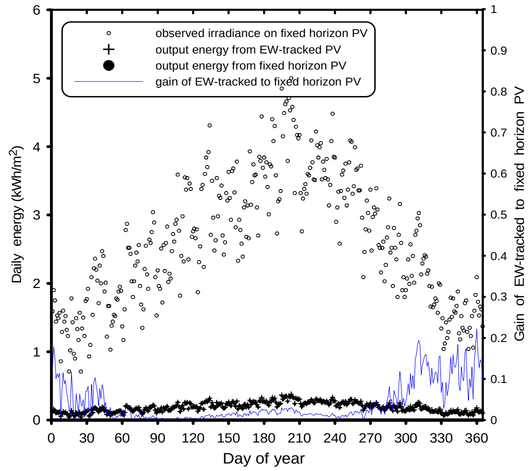

Figure 9. EW-tracked PV's daily performance according to observed radiation

Figure 11 shows the yearly output energy of PV as a function of the maximum rotation angle of tracked panel.

It can be seen that the energy increases with the rotation angle, but the benefit of employing a sun-tracking system in real environment like in Taipei is not as good as in clear sky. This is true because the benefit that might be improved by a sun-tracking system depends greatly on the level of direct beam.

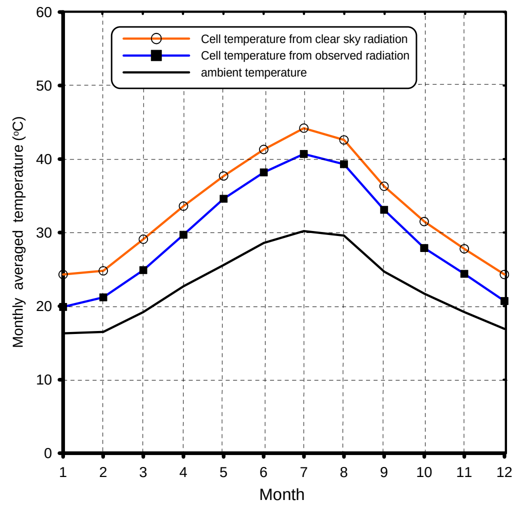

Figure 10. Monthly averaged temperature

The fraction of beam radiation becomes lower if the sky clearness index decreases, e.g. in an overcast day. Meanwhile the curve slope becomes gentler when the rotation angle increases implying that the tracking benefit becomes less significant. With the maximum rotation angle of 45^o used by the present study (as marked with a vertical broken line), the yearly gains of output energy obtained by the tracked panel are 14.1% and 5.5% for clear sky and observed radiation, respectively. Basically the gains calculated from electrical energy are close to those from irradiance.

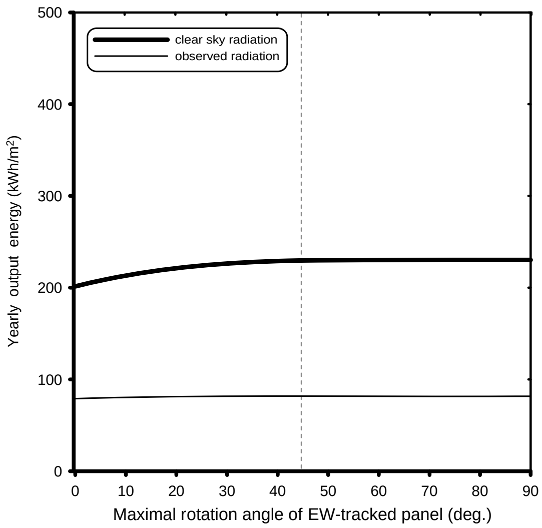

Figure 11. Variation of yearly output energy from EW-tracked PV with the maximum rotation angle of panel

5. Conclusion

In this paper, the performance of EW-tracked panel is investigated; electrical energy output from a mono-crystalline silicon photovoltaic module is simulated according to the radiation observed and the one predicted under clear sky environment in Taipei. The conclusions are summarized as follows:

(1) EW-tracked panel would generate more power near noon due to its smaller incident angle of sunlight, which is useful for special solar design.

(2) The tracked panel makes a greater gain in winter but worse in summer for the changes of the Sun's elevation.

(3) The output energy from tracked PV under real environment as in Taipei is quite less than that under clear sky. The yearly conversion efficiency of PV is 9.1% and 8.2% for clear sky and observed radiation, respectively.

(4) The output energy of PV module increases with its maximum rotation angle, with 45^o of maximum rotation angle the annual gains obtained are 14.1% and 5.5% for clear sky and observed radiation, respectively.

Acknowledgments

The author would deeply appreciate the Central Weather Bureau for providing irradiance data and thank Dr. Huang MW, researcher of the Institute of Earth Sciences, Academia Sinica, Taiwan, for his treasure suggestions. This work was supported in part by Nankai University of Technology.

Notations

A ideality factor, dimensionless

C_i temperature coefficient, mA/ oK

dn day number of year, dimensionless

E_g semiconductor gap energy, eV

I output current of solar cell, A

I_c clear sky radiation on horizontal surface, J/m2

I_{cb} clear sky beam on horizontal surface, J/m2

I_{cd} clear sky diffusion on horizontal surface, J/m2

I_d bypass diode current, A

I_{ph} photo-induced current, A

I_{rr} reverse saturation current at reference temperature, A

I_{sat} reverse saturation current, A

I_{scr} short circuit current, A

I_t global radiation on tilted panel, J/m2

K Boltzmann constant, 1.380658*10-23

$\bar{M}$ unit normal vector of EW-tracked panel
$\bar{M}'$ unit vector perpendicular to and lagging behind the normal vector of EW-tracked panel by 90o
$\bar{P}$ unit vector of the Sun's apparent position
q magnitude of electron charge, 1.602*10-19 C
R_b beam radiation ratio, dimensionless
S solar radiation, kW/m2
T cell temperature, oK
T_a ambient temperature, oK
T_r reference temperature, oK
V output voltage of solar cell, V

Greek letters

γ rotation angle of panel, degrees
δ solar declination, degree
ω solar hour angle, degree
θ_{ew} incident angle of sunlight to EW-tracked panel, degrees
θ_z zenith of the Sun, degree
ϕ geographic latitude, degree
ψ azimuth of the Sun, degree
ρ reflection coefficient, dimensionless

References

[1] Luque, A., and Hegedus, S. 2002. Handbook of Photovoltaic Science and Engineering. John Wiley & Sons Ltd. 87-111.
[2] Chen, Y. M., Lee, C. H., and Wu, H. C. 2005. Calculation of the optimum installation angle for fixed solar-cell panels based on the genetic algorithm and the simulated-annealing method. IEEE Trans. on Energy Conversion, 20, 2: 467-473.
[3] Chan, D. S. H., Phillips, J. R., and Phang, J. C. 1986. A comparative study of extraction methods for solar cell model parameters. Solid-state Electronics, 29: 329-337.
[4] Markvart, T. 2000. Solar Electricity, 2nd edition. John Wiley & Sons Ltd. 5-18.
[5] Fan, Y. C., Lee, T. P., Kuo, S. W., Lo, Y. K., and Chiu, H. J. 2008. Single-stage DC power supply by paralleling the utility and a photovoltaic system at DC side. The 7th conference & exhibition of power electronics in Taiwan, 660-665.
[6] Morcos, V. H. 1994. Optimum tilt angle and orientation for solar collectors in Assiut, Egypt. Renewable Energy, 4, 3: 291-298.
[7] Neville, R. C. 1978. Solar energy collector orientation and tracking mode. Solar Energy, 20, 1: 7-11.
[8] Huang, B. J. and Sun, F. S. 2007. Feasibility study of one axis three positions tracking solar PV with low concentration ratio reflector. Energy Conversion and Management, 48: 1273-1280.
[9] Abdallah, S. 2004. The effect of using sun tracking systems on the voltage–current characteristics and power generation of flat plate photovoltaics. Energy Conversion and Management, 45: 1671-1679.
[10] Al-Mohamad, A. 2004. Efficiency improvements of photo-voltaic panels using a Sun-tracking system. *Applied Energy,* 79, 3: 345-354.
[11] Sungur, C. 2009. Multi-axes sun- tracking system with PLC control for photovoltaic panels in Turkey. Renewable Energy, 34: 1119–1125.
[12] Liu, C. M. 1996. Climate and weather in Taiwan. Formosa Folkways Publishing Company, Taipei, Taiwan.
[13] Liu, C. M., Shen, S. L. and Feng, S. T. 1990. Cloud effect on the round- measured downward global solar flux: analysis and parameterization. Atmospheric Sciences, 18: 35-55.

[14] Liu, C. M. and Fong, C. S. 1989. The analysis of aerosol attenuation on surface direct solar flux. Atmospheric Sciences, 17: 169-186.
[15] Feng, S. T., Liu, C. M. and Sheng, C. L. 1989. The extinction of global solar flux by aerosol. Atmospheric Sciences, 17: 287-302.
[16] Chang, T. P. 2009. Performance study on the east-west oriented single-axis tracked panel. Energy, 34, 10: 1530-1538.
[17] Cheng, C. L., Chan, C.Y. and Chen, C. L. 2006. An empirical approach to estimating monthly radiation on south-facing tilted planes for building application. Energy, 31: 2940-2957.
[18] Chang, T. P. 2009. Performance evaluation for solar collectors in Taiwan. Energy, 34, 1: 32-40.
[19] Hussein, H. M. S., Ahmad, G.. E. and El-Ghetany, H. H. 2004. Performance evaluation of photovoltaic modules at different tilt angles and orientations. Energy Conversion and Management, 45: 2441-2452.